

THE COSMIC EVOLUTION OF AGN IN GALAXY CLUSTERS

AUDREY GALAMETZ^{1,2,3}, DANIEL STERN¹, PETER R. M. EISENHARDT¹, MARK BRODWIN⁴,
MICHAEL J. I. BROWN⁵, ARJUN DEY⁴, ANTHONY H. GONZALEZ⁶, BUELL T. JANNUZI⁴,
LEONIDAS A. MOUSTAKAS¹, S. ADAM STANFORD⁷

Draft version October 29, 2018

ABSTRACT

We present the surface density of luminous active galactic nuclei (AGN) associated with a uniformly selected galaxy cluster sample identified in the 8.5 square degree Boötes field of the NOAO Deep Wide-Field Survey. The clusters are distributed over a large range of redshift ($0 < z < 1.5$) and we identify AGN using three different selection criteria: mid-IR color, radio luminosity, and X-ray luminosity. Relative to the field, we note a clear overdensity of the number of AGN within 0.5 Mpc of the cluster centers at $z > 0.5$. The amplitude of this AGN overdensity increases with redshift. Although there are significant differences between the AGN populations probed by each selection technique, the rise in cluster AGN surface density generally increases more steeply than that of field quasars. In particular, X-ray selected AGN are at least three times more prevalent in clusters at $1 < z < 1.5$ compared to clusters at $0.5 < z < 1$. This effect is stronger than can be explained by the evolving median richness of our cluster sample. We thus confirm the existence of a Butcher-Oemler type effect for AGN in galaxy clusters, with the number of AGN in clusters increasing with redshift.

Subject headings: galaxies: active - galaxies: clusters: general - galaxies: evolution - infrared: galaxies - X-rays: galaxies - radio continuum: galaxies

1. INTRODUCTION

In the local universe, AGN are known to be much less common in rich galaxy cluster environments as compared to the field. Optical observations dating back more than three decades show that while 5% of massive field galaxies show spectroscopic signatures of nuclear activity, only 1% of the corresponding population in local galaxy clusters show such signatures (Dressler et al. 1985). Assuming that the $M_{\bullet} - \sigma$ relation (e.g., Magorrian et al. 1998) holds in rich environments, this suggests that the supermassive black holes hosted by massive cluster galaxies are currently quiescent or their nuclear activity is optically obscured. In addition, the intracluster plasma in rich galaxy clusters is maintained at high temperatures; AGN feedback has been suggested as the most natural heat source by numerous authors (e.g., McNamara et al. 2000; Birzan et al. 2004). This suggests that the activity level of AGN in cluster galaxies, and their influence on the formation and evolution of clusters, may have been higher in the past.

Early studies of AGN in clusters largely relied on optical spectroscopy (e.g., Bahcall et al. 1969), a technique which is notoriously insensitive to both obscured and

low luminosity AGN. In contrast, multi-wavelength approaches provide a significantly more thorough census of AGN. For example, Compton-thick, luminous AGN will be faint at the relatively low (< 10 keV) energies probed by *Chandra* and *XMM/Newton* and would be unlikely to show a UV-excess or spectroscopic signatures of nuclear activity at cosmological distances. Such sources would be easier to identify at radio or mid-IR energies, though only a $\sim 10\%$ of AGN are radio-loud. We briefly review selection of AGN at non-optical wavelengths, summarizing previous work using these techniques to study the cosmic evolution of AGN in galaxy clusters.

X-Ray Selected AGN. In the past decade, sensitive X-ray observatories have provided an efficient method to identify AGN. Several studies conducted on individual clusters or small cluster samples have shown an excess of X-ray point sources in galaxy clusters (Cappi et al. 2001; Eckart et al. 2006). Martini et al. (2002, 2006, 2007) study samples of X-ray sources near low-redshift galaxy clusters with spectroscopic follow-up to confirm cluster membership. Similar to field X-ray source studies, this work has shown that X-ray emitting galaxies in clusters often do not show AGN signatures in their optical spectra, implying that a significant fraction of cluster nuclear activity is optically obscured. Considering a sample of four galaxy clusters at $z \sim 0.6$, Eastman et al. (2007) show that the X-ray AGN are more common at $z \sim 0.6$ than at $z \sim 0.2$, implying that the cluster AGN fraction increases rapidly with redshift.

Other groups have foregone spectroscopic observations and have looked for enhancements in the radial distribution of X-ray sources around clusters. For example, Ruderman & Ebeling (2005) derive the surface density profile of X-ray sources around a sample of 51 galaxy clusters at $0.3 < z < 0.7$ from the *Chandra* MASSive Cluster Survey (MACS; Ebeling et al. 2001). They find that X-ray sources show a very pronounced central spike

¹ Jet Propulsion Laboratory, California Institute of Technology, 4800 Oak Grove Dr., Pasadena, CA 91109, [e-mail: agalamet@eso.org]

² European Southern Observatory, Karl-Schwarzschild-Str. 2, D-85748 Garching, Germany

³ Observatoire Astronomique de Strasbourg, 11 rue de l'Université, 67000 Strasbourg, France

⁴ National Optical Astronomy Observatory, 950 North Cherry Avenue, Tucson, AZ 85719

⁵ School of Physics, Monash University, Clayton, Victoria 3800, Australia

⁶ Department of Astronomy, University of Florida, Gainesville, FL 32611

⁷ Institute of Geophysics and Planetary Physics, Lawrence Livermore National Laboratory, Livermore, CA 94550

($r < 0.5$ Mpc) and a second excess at ~ 2.5 Mpc relative to the cluster centers. They suggest the former is from nuclear activity triggered by infalling galaxies approaching the central giant elliptical galaxy, while the second peak, which is most pronounced in virialized clusters, is due to galaxy mergers at the cluster-field interface. Bignamini et al. (2008) find an excess of X-ray point sources near the centers of optically-selected clusters at $0.6 < z < 1.2$.

Radio Selected AGN. Over the past 50 years there have been numerous studies of the environments of powerful radio galaxies which are now well known to often be associated with the central member of galaxy clusters, not only at low redshifts (Matthews et al. 1964) but also at high redshifts (Dickinson 1993; Stern et al. 2003; Miley et al. 2004; Venemans et al. 2005, 2007, Galametz et al., in prep.). Correlating the Sloan Digital Sky Survey (SDSS; Gunn & Weinberg 1995) with the Faint Images of the Radio Sky at Twenty cm survey (FIRST; Becker et al. 1995), Best et al. (2005) show that there is a strong tendency for low-redshift radio-loud galaxies to be found in rich environments. Lin & Mohr (2007) derive the radio-loud AGN density profile from a sample of 573 nearby ($z \leq 0.2$) X-ray selected galaxy clusters and find a clear excess of AGN in the center of the galaxy clusters. Croft et al. (2007), studying brightest clusters galaxies (BCGs) at $z < 0.3$ from a sample of 13,240 galaxy clusters, report that 19.7% of BCGs are detected in the radio, with the majority of these (92.8%) being radio-loud ($L_{1.4\text{GHz}} \geq 10^{23}$ W Hz $^{-1}$). In contrast to these studies of X-ray and radio-selected AGN in galaxy clusters, optically-selected, luminous quasars exhibit clustering comparable to that of local field galaxies, and therefore primarily reside in lower mass dark matter halos (e.g., Croom et al. 2005; Coil et al. 2007).

Mid-IR Selected AGN. AGN can also be efficiently identified using mid-infrared colors (Lacy et al. 2004; Stern et al. 2005). While the optical to mid-infrared ($\lambda \leq 5\mu\text{m}$) continuum of normal galaxies is dominated by the composite stellar black body emission and peaks at approximately $1.6\mu\text{m}$, the optical to mid-infrared continuum of active galaxies is dominated by a power law. Consequently, with sufficient wavelength baseline, one can easily distinguish AGN from stellar populations. Little work has been done to date on the prevalence of mid-IR selected AGN in clusters, though Hickox et al. (submitted) shows that low redshift ($z < 0.8$) mid-IR selected AGN have weaker clustering properties (e.g., smaller correlation lengths) than either X-ray or radio-selected AGN. At high redshift ($z \sim 2$), however, various mid-infrared AGN samples show strong clustering, suggesting that they are preferentially associated with clusters (Brodwin et al. 2008; Dey et al. 2008; Magliocchetti et al. 2008).

Previous studies of AGN activity in galaxy clusters have typically focussed on a single selection technique, generally over a limited redshift range and with a limited cluster sample size. Combining the IRAC Shallow Survey (ISS; Eisenhardt et al. 2004) and the *Chandra* XBoötes Survey (Murray et al. 2005), Gorjian et al. (2008) compare mid-IR and X-ray AGN selection and find that only 28% of XBoötes sources are selected by the Stern et al. (2005) mid-infrared criteria. On the

other hand, a significant number (43%) of AGN selected in mid-infrared have an X-ray counterpart in XBoötes (V.Gorjian, private communication). Furthermore, only $\sim 10\%$ of optically-selected luminous quasars are radio-loud (e.g., Stern et al. 2000). These results imply that to obtain the fullest census of nuclear activity, multiple AGN selection techniques are required.

In this paper, we present the surface density of AGN selected by three techniques (mid-infrared color, radio luminosity, and X-ray luminosity) in a large sample of uniformly-selected galaxy clusters identified in the Boötes field (Eisenhardt et al. 2008). The next section (§2) describes the galaxy cluster and AGN samples. We describe the radial surface density profile of AGN in galaxy clusters in §3 and discuss the results in §4. We assume a Λ CDM cosmology with $H_0 = 70$ km s $^{-1}$ Mpc $^{-1}$, $\Omega_m = 0.3$ and $\Omega_\Lambda = 0.7$.

2. THE GALAXY CLUSTER AND AGN SAMPLES

The galaxy cluster sample we analyze has been uniformly selected from the 8.5 square degree ISS field in Boötes survey, which has been observed by a wide array of facilities at multiple wavelengths. The following sections describe first the cluster sample and then AGN samples identified in the Boötes field at mid-infrared, radio and X-ray energies. Note that in the later analysis (§3), we will use these AGN samples, generally from flux-limited catalogs, to study the cosmic evolution of AGN in galaxy clusters. To ensure uniformity in the analysis, this will entail creating luminosity-selected sub-samples (§3).

2.1. The IRAC Shallow Survey cluster sample

Eisenhardt et al. (2008) present a sample of 335 galaxy clusters identified in the Boötes field of the NOAO Deep Wide-Field Survey (NDWFS; Jannuzi & Dey 1999). The clusters, reaching out to redshift $z = 2$, were identified by combining ISS with *B_WRI* imaging from the NDWFS and *JK_s* imaging from the FLAMINGOS Extragalactic Survey (FLAMEX; Elston et al. 2006). Brodwin et al. (2006) calculated photometric redshifts for $4.5\mu\text{m}$ -selected sources in the ISS. Clusters were then identified using a wavelet algorithm which identified three-dimensional overdensities of galaxies (in 2 angular dimensions) with comparable photometric redshifts. The clusters have average halo masses of $\sim 10^{14}$ M_\odot (Brodwin et al. 2007). The cluster centers were determined from their peaks in the wavelet detection map. Since this map is based on the positions of a limited number of galaxies per cluster, the cluster center accuracy is expected to be comparable to the 12'' resolution of the wavelet map.

An estimate of the cluster redshifts was obtained from the photometric redshift probability distribution of candidate cluster members. At $z < 0.5$, 67 of the 91 clusters candidates are confirmed by the AGN and Galaxy Evolution Survey (AGES; Kochanek et al., in prep.), which provides spectroscopic redshifts for ~ 17000 objects in the ISS. To date, 12 of the $z > 1$ cluster candidates have been confirmed spectroscopically (Stanford et al. 2005; Elston et al. 2006; Brodwin et al. 2006; Eisenhardt et al. 2008). Where available, we use the spectroscopically determined cluster redshifts. For the remaining cluster sample, we use the best fit photometric redshift which

includes a small, empirically-determined offset relative to the mean photometric redshift of the candidate cluster members. This large, uniformly selected galaxy cluster sample is spread over a large range of cosmic time and thus provides a powerful tool for studying the dependence of the AGN distribution on both redshift and environment.

2.2. Mid-IR selected AGN

Using mid-infrared colors, provided by the ISS, of nearly 10,000 spectroscopically identified sources from AGES, Stern et al. (2005) show that AGN can robustly be identified from their IRAC colors (see also Lacy et al. 2004; Donley et al. 2008). Simple mid-infrared color criteria select over 90% of the spectroscopically identified type 1 AGN and 40% of the type 2 AGN. The selection relies on the fact that while stellar populations fade longward of their $1.6\mu\text{m}$ peak, luminous AGN exhibit red power-law emission throughout the mid-infrared. Notably, this power-law long wavelength emission is relatively immune to gas and dust absorption, making mid-infrared AGN selection sensitive to both obscured and unobscured luminous AGN, relatively independent of redshift. We note however that this selection fails for low-luminosity AGN where the host galaxies contributes much of the mid-IR flux (Eckart et al., in prep.). We extract all 2262 sources selected by the Stern et al. (2005) criteria that are well detected (5σ) in all four IRAC bands. For a typical AGN spectral energy distribution, the $5.8\mu\text{m}$ band is the least sensitive, with a 5σ limiting depth of $51\mu\text{Jy}$ ($3''$ diameter aperture). We find a mean surface density of 283 mid-infrared selected AGN candidates per square degree in the Boötes field.

2.3. Radio selected AGN

Several shallow ($\geq 1\text{mJy}$) radio surveys have covered the ISS field at 1.4 GHz, including the NRAO VLA Sky Survey (NVSS; Condon et al. 1998) and FIRST. More recently, the Westerbork Synthesis Radio Telescope (WSRT) has covered approximately 6.68 square degrees of Boötes, reaching a 1σ limit of $28\mu\text{Jy}$ at 1.4 GHz (de Vries et al. 2002). The final catalog of 5σ detected sources contains 3172 objects¹, corresponding to a surface density of 453 radio sources per square degree.

The brightest radio sources in the sky tend to be AGN, with their radio emission dominated by synchrotron radiation. However, sufficiently deep radio surveys are also able to detect radio emission associated with stellar processes such as supernova explosions and compact stellar remnants, abundant in star-forming galaxies. Condon (1992) shows that for these star forming galaxies, the star formation rate (SFR) is proportional to the radio emission. Following Condon et al. (1992), Serjeant, Grappioni & Oliver (2002) obtain $L_{1.4\text{GHz}}(\text{erg s}^{-1} \text{Hz}^{-1}) = 8.2 \times 10^{27} \times \text{SFR}(M_{\odot} \text{yr}^{-1})$. Submillimeter galaxies correspond to the objects with the highest known SFR, reaching $\text{SFR} \sim 1000M_{\odot} \text{yr}^{-1}$ (Pope et al. 2006). We conservatively assume that no galaxy has a SFR greater than $3000M_{\odot} \text{yr}^{-1}$ and thus any radio source with a 1.4 GHz luminosity density greater than $2.46 \times 10^{31} \text{erg s}^{-1} \text{Hz}^{-1}$

must host an AGN (see §3). Given the depth of the WSRT observations, all radio-loud AGN in the Boötes field should be detected out to redshift $z \sim 3.7$.

2.4. X-ray selected AGN

XBoötes is the largest contiguous survey with the *Chandra X-Ray Observatory*. It consists of 9 square degrees of imaging of the NDWFS Boötes field, comprised of 126 5 ks pointings, with a corresponding depth of $\sim 7.8 \times 10^{-15} \text{ergs cm}^{-2} \text{s}^{-1}$ in the 0.5-7 keV band. The X-ray catalog consists of 3293 point sources with four or more X-ray counts (366 sources per square degree; Kenter et al. 2005; Brand et al. 2006) and is publicly available². At the shallow depth of these data, the majority of the X-ray sources are expected to be AGN. Indeed, based on AGES optical spectra for 892 XBoötes sources (Kenter et al. 2005), AGN represent at least 69% of the sources with spectra. Only 3% of the sources are identified as stars. The remaining 28% lack obvious AGN features in their optical spectra but are suspected to be AGN based on their X-ray luminosities. XBoötes is only sensitive to starbursts out to $z = 0.12$ (e.g., see Gorjian et al. 2008). Since only one of the galaxy clusters in the ISS sample is at $z < 0.12$, we consider the possible influence of X-ray detected starbursts negligible in this work.

3. RADIAL SURFACE DENSITY PROFILE OF AGN

In order to study the cosmic evolution of AGN in galaxy clusters, we opt for a simple empirical approach: we calculate the radial distribution of AGN around galaxy clusters as a function of cluster redshift, with AGN identified using the three selection criteria described above. We separate the ISS clusters into three redshift bins: $0 < z \leq 0.5$, $0.5 < z \leq 1$ and $1 < z \leq 1.5$, resulting in 91, 140 and 79 clusters per bin, respectively, for the mid-IR and X-Ray techniques. The remaining 25 clusters are at $z > 1.5$, and are thus ignored in this work. The area covered by the WSRT radio data is smaller than the ISS and thus only 285 clusters have deep coverage at radio wavelengths. Of these 285 clusters, 77, 121 and 69 are found at $0 < z \leq 0.5$, $0.5 < z \leq 1$ and $1 < z \leq 1.5$, respectively.

In order to ensure that similar populations are plotted in each cluster redshift bin, we apply uniform luminosity cuts to the data. In detail, since most of the sources considered here lack spectroscopic redshifts, for a given cluster at redshift z , we only consider sources brighter than some evolving flux density such that their luminosity would be equal to or above our luminosity limit assuming that the source were in the cluster. For the very sensitive radio survey, we apply the luminosity cut $S_{1.4\text{GHz}} > 2.5 \times 10^{40} \text{ergs s}^{-1}$ (see §2.3) to isolate AGN from star-forming galaxies. For the mid-IR and X-ray selected AGN, we apply a luminosity cut corresponding to the flux limit of the corresponding surveys at $z = 1$ (see §3.1 and 3.3 for details). This redshift is selected as a compromise between obtaining sufficient numbers of AGN, large numbers of clusters, and sufficient leverage on the cosmic time probed. Table 1 presents the number of sources that remain for each selection technique

¹ The catalog as well as the mosaic can be obtained through anonymous ftp to <ftp://ftp.nfra.nl/pub/Bootes>.

² <http://heasarc.nasa.gov/W3Browse/all/xbootes.html>

and redshift bin. These numbers are based on cuts (described in detail in the following subsections) corresponding to the median redshift of the clusters in each bin, e.g., $\langle z \rangle = 0.38$ (0.39), $\langle z \rangle = 0.74$ (0.74) and $\langle z \rangle = 1.19$ (1.18) for mid-IR and X-ray (radio) selections. Also tabulated are the field AGN surface densities for each technique and redshift bin, where we have simply divided the number of sources by the corresponding survey area. These field surface densities are shown as dashed horizontal lines in Fig. 1. Finally, we note that for the X-ray and mid-IR selected AGN in the highest redshift bin ($1 < z \leq 1.5$), this approach only provides a lower limit to the surface density of AGN down to the luminosity limit considered in the lower redshift bins.

The surface density distributions for AGN in the galaxy clusters are calculated as follows. We calculate the angular separation from each ISS cluster center to each mid-infrared, radio and X-ray selected AGN candidate, subject to the flux cuts discussed above. AGN candidates are identified out to $5'$ from the cluster centers, and we bin the radial distances to compute the surface density profiles of AGN ($0.5'$ bins), presented in Fig. 1. As expected, at large radii the derived surface densities asymptote to the field AGN surface densities. Throughout this paper, we adopt Poissonian errors for AGN counts and use the Gehrels (1986) small numbers approximation for Poisson distributions. Fig. 1 presents the 1σ errors for both the AGN counts and the field surface densities for each technique and redshift bin.

As a check on this method, we also calculated the AGN surface density distribution at random locations in the field. We created 40 mock cluster samples by simply offsetting all of the cluster positions by medium-scale offsets — larger than the typical cluster size, but small enough that few clusters would fall outside of the survey region. Deriving the radial surface density profile around the mock cluster samples, we consistently find no significant variation relative to the field surface densities.

In contrast to the mock sample, an excess of AGN is found near the centers of clusters, most prominently at $z \geq 0.5$. The next sections detail the results obtained for each of the three AGN selection criteria considered. We note that we have verified that spatially proximate clusters are not biasing our results. Since the overdensities described below are only found at small radii (< 1 Mpc), the number of AGN counted as potential central members to more than one cluster is negligible (null for $r < 0.5$ Mpc, and $< 1\%$ for $0.5 < r < 1$ Mpc).

3.1. Density profile of mid-IR selected AGN

The radial surface density profile for mid-IR selected AGN is shown in Fig. 1 (top row), separated into the three redshift bins described above. The $5.8\mu\text{m}$ limiting flux density of the ISS is $51\mu\text{Jy}$ (5σ). Assuming a pure power law spectrum for the AGN, the corresponding luminosity density is $L_\nu = 4\pi d_L^2 S_\nu / (1+z)^{(1-\alpha)}$ where d_L is the luminosity distance and α is the spectral index ($S_\nu \propto \nu^\alpha$). This assumption of a power-law is born out by both the mid-IR color-color plots of broad-lined AGN used to develop the mid-IR AGN selection criteria (e.g., Lacy et al. 2004, Stern et al. 2005) and broad-band composite AGN spectral energy distributions (Richards et al. 2006). We adopt a mean spectral index of 0.73, as given by Stern et al. (2005). The

depth of the ISS $5.8\mu\text{m}$ data corresponds to a $5.8\mu\text{m}$ luminosity of 2.2×10^{44} ergs s^{-1} at $z = 1$, which we adopt as our luminosity cut. Thus for any given cluster we only consider mid-IR selected AGN whose luminosity (and corresponding flux density) is above this value under the assumption that they are at the cluster redshift.

The $z \leq 0.5$ galaxy clusters do not show any significant enhancement of mid-IR selected AGN relative to the field. In the $0.5 < z \leq 1$ bin, however, a weak overdensity of mid-IR selected AGN is observed at the cluster center ($r < 0.3$ Mpc). Throughout the paper, the significance of overdensities have been derived as follows. We first subtract the number of AGN in a given aperture by the field AGN population to a given (redshift-dependent) flux density limit. This field-corrected number of AGN is then referenced to the expected field counts using the Gehrels (1986) small numbers approximation for Poisson distributions. The central excess of $0.5 < z \leq 1$ mid-IR selected AGN is thus significant at the 2σ level. A small excess of AGN is suggested in the center of the $z > 1$ galaxy clusters, but is not significant relative to the field density. Recall that since the highest redshift bin considers more luminous AGN than the $z < 1$ bins, the resulting, weak overdensity is a lower limit to the number of AGN per cluster to the luminosity limit of the $z < 1$ clusters.

3.2. Density profile of radio selected AGN

The radial surface density profile for radio-selected AGN is shown in Fig. 1 (middle row), separated into three redshift bins. For each redshift bin, we apply the conservative uniform luminosity cut described in §2.3 to remove star-forming galaxies, adopting a mean radio spectral index of -0.75 , as given in de Vries et al. (2002).

In the $z \leq 0.5$ bin, a weak overdensity (1.5σ) of radio sources is observed at the cluster center. The $0.5 < z \leq 1$ galaxy clusters show a very clear excess of AGN in the center ($r < 0.3$ Mpc), with no excess seen at larger radii. The central excess is significant at the 3σ level. The higher redshift galaxy clusters ($1 < z \leq 1.5$) also show a significant excess (2σ) at the cluster center, albeit weaker and on a larger scale ($r < 0.5$ Mpc) relative to the moderate redshift galaxy clusters.

3.3. Density profile of X-ray selected AGN

The radial surface density profile for X-ray selected AGN is shown in Fig. 1 (bottom row). The limiting flux of XBoötes in the $0.5 - 7.0$ keV range is $\sim 7.8 \times 10^{-15}$ ergs cm^{-2} s^{-1} , where the XBoötes flux values have been calculated from the counts assuming an X-ray AGN power-law spectrum with photon index $\Gamma = 1.7$ (Kenter et al. 2005). While the shallow depth of the XBoötes survey implies that any source detected at $z \geq 0.12$ must be an AGN (Gorjian et al. 2008), we only plot sources whose X-ray luminosity exceeds the limiting sensitivity of XBoötes at redshift unity. The same photon index value is adopted to calculate the X-ray luminosities. The luminosity cut applied for X-ray selection is therefore 3.3×10^{43} ergs s^{-1} in the $0.5 - 7.0$ keV range. As emphasized for the mid-IR selected AGN, the lower, right panel of Fig. 1 is a lower limit to the surface density of X-ray selected AGN at the luminosities plotted in the first two panels.

No significant enhancement of the X-ray selected AGN is observed for the lowest redshift ($z \leq 0.5$) galaxy clusters. A small central overdensity is suggested for $0.5 < z \leq 1$ galaxy clusters (1.2σ level; $r < 0.5$ Mpc). On the other hand, the $1 < z \leq 1.5$ galaxy clusters show a modest excess (2σ) at the cluster center ($r < 0.25$ Mpc).

We note that, in principle, X-ray point sources are harder to identify in galaxy clusters with significant diffuse X-ray emission. The intergalactic medium in such clusters would tend to decrease the apparent AGN surface density for lower redshift clusters in a shallow survey such as XBoötes. XBoötes identifies 43 extended sources (Kenter et al. 2005) of which 38 are covered by ISS. The size of these extended sources, derived from Gaussian fits to their source profiles, is (except for one source) less than $0.5'$. The overdensity of X-ray point sources that we observe in our galaxy cluster sample is clearly detected within 0.5 Mpc ($r \sim 1.5'$ at $z = 0.5$) of the cluster center. The brightness of an unresolved cluster member with an X-ray luminosity equivalent to our threshold would, on average, be five times brighter than that of the extended sources. Only in four clusters would a threshold source have a flux comparable to the extended source (e.g., brightness contrast < 2). Given these small numbers, we are confident that extended, diffuse X-ray emission from rich clusters is not strongly biasing our results.

4. DISCUSSION

This paper presents the first comprehensive study of the radial density profile of AGN for a uniformly-selected cluster sample distributed over a large fraction of cosmic time. Only the radio-selected AGN show a weak (1.5σ) overdensity in the lowest redshift ($z \leq 0.5$) bin. An excess of AGN is observed near the center ($r < 0.5$ Mpc) of galaxy clusters at $z > 0.5$, and all three AGN selection criteria show a pronounced enhancement in AGN activity at $0.5 < z \leq 1$ relative to $z \leq 0.5$. The excess is even observed for the highest redshift galaxy clusters ($1 < z \leq 1.5$), though we are only plotting to the flux limits of the input mid-IR and X-ray catalogs at these high redshifts, implying a less sensitive luminosity limit than in the $z \leq 1$ clusters. We therefore show that AGN activity in galaxy clusters increases with redshift.

We first compare the luminosity cuts applied for each selection criteria to see how the AGN samples relate to one another. The luminosity cut applied for the mid-infrared selection is 2.2×10^{44} ergs s^{-1} at $5.8\mu\text{m}$. Elvis et al. (1994) provides a mean spectral energy distribution (SED) for quasars derived from broad-band photometry covering the full electromagnetic spectrum from radio to X-rays. Using this composite SED for radio-loud quasars, the luminosity cut at $5.8\mu\text{m}$ corresponds to a luminosity cut of $\sim 2.2 \times 10^{43}$ ergs s^{-1} in the 0.5–7 keV X-ray band and 2.2×10^{41} ergs s^{-1} at 1.4 GHz. Our X-ray luminosity cut is 3.3×10^{43} ergs s^{-1} which is comparable to the depth of the mid-infrared selection. A more recent determination of the mean quasar SED was performed by Richards et al. (2006) and gives an X-ray luminosity five times smaller at a given mid-infrared luminosity compared to the Elvis et al. (1994) template. This would imply that our X-ray selection only identifies AGN five times more powerful than the mid-infrared selection. Our radio luminosity cut is 2.5×10^{40} ergs s^{-1}

at 1.4 GHz. Therefore, the AGN radio selection depth is reaching almost ten times the depth of the mid-infrared selection, and ten to fifty times the depth of the X-ray selection, depending on which quasar composite template is adopted. This deeper radio sensitivity is a plausible explanation for why only the radio-selected AGN show an overdensity in the lowest redshift galaxy clusters.

One concern is that due to the larger volumes accessible at higher redshifts, our sample of clusters becomes progressively richer with redshift. In this case, the rising number of AGN seen in the higher redshift clusters could simply trace the rising number of massive cluster members in the higher redshift clusters, with a constant, non-evolving fraction of massive galaxies being active. In order to study this effect, we use the photometric redshifts derived from the $4.5\mu\text{m}$ ISS sample (see §2.1) to determine the mean number of cluster members brighter than $0.5L^*$ as a function of cluster redshift. We consider the observed $3.6\mu\text{m}$ flux density, converted to $1.6\mu\text{m}$ rest-frame luminosity assuming a $z_f = 3$ formation redshift and passive evolution (e.g., see Eisenhardt et al. 2008). We only consider members brighter than $0.5L^*$ within the inner 0.5 Mpc of the clusters. As expected, we do indeed find clusters at $z \sim 0.3$ are, on average, slightly less rich than clusters at $z \sim 0.8$. Clusters at $0 < z \leq 0.5$ have an average of 6.5 members brighter than $0.5L^*$ while 10.0 members are found, on average, in clusters at $0.5 < z \leq 1$. At redshifts above 0.8, the number of cluster members in the inner 0.5 Mpc and brighter than $0.5L^*$ actually begins to decrease, with 5.7 galaxies, on average, for clusters at $z > 1$. This is not a sensitivity issue since the 90 seconds of combined exposure of ISS provides sufficient sensitivity to detect evolving L^* galaxies to $z = 2$ (Eisenhardt et al. 2008). This decrease in cluster member numbers instead could reflect that clusters at $z > 0.8$ are still in the process of collapsing, that the clusters members are merging, or some combination thereof. However, the variation with redshift is only at the 50% level, while the cosmic evolution of AGN activity is a factor of several more significant (with some variation depending on which AGN selection criterion has been used). For the following discussion, we therefore omit the modest systematic dependence of cluster richness on redshift inherent to the Boötes cluster sample. We do note, however, that this trend would serve to make the fraction of active galaxies in the central regions of $z > 1$ clusters even higher relative to the fraction at $z < 0.8$, since the number of AGN is rising while the number of luminous cluster members is falling.

It is well known that AGN are more common at high redshift. Indeed, there is a strong increase in the quasar density with redshift from the local universe out to $z \sim 2$, a result that dates back four decades (Schmidt 1968). Since then, numerous studies have determined the quasar luminosity function (QLF) for radio (e.g., Dunlop & Peacock 1990), optical (e.g., Croom et al. 2004), infrared (e.g., Brown et al. 2006) and X-ray AGN samples (e.g., Ueda et al. 2003). Eastman et al. (2007) find that the cluster AGN fraction at $z \sim 0.6$ is approximately a factor of 20 greater than the cluster AGN fraction at $z \sim 0.2$. In comparison, this increase is only 1.5 (3.3) for the field sample of AGN more luminous than $L_x > 10^{42}$ (10^{43}) ergs s^{-1} over this redshift range. In order to compare the

AGN overdensities associated with galaxy clusters, seen in Fig. 1, to the field AGN population, we derive average cluster AGN volume densities as follows. We count the number of sources projected within 0.25 Mpc of the cluster centers for the various redshift bins and selection criteria, and then field-correct this number by subtracting the expected number of sources over this same area based on the field surface density. We assume any identified overdensity is associated with the cluster (e.g., is neither foreground nor background). For the sake of simplicity, we assume a spherical distribution at the cluster redshift to derive a volume density from the measured (field-corrected) surface density. Fig. 2 presents this field-corrected volume density of AGN within 0.25 Mpc of the galaxy clusters in the three redshift intervals and for the three AGN selection criteria. We also plot the evolution of optically-selected quasars over this same redshift range using the QLF derived by Croom et al. (2004) from the 2dFQZ project³. At $z = 1$, Croom et al. (2004) find that $L_{\text{AGN}}^* = 1.6 \times 10^{45} \text{ erg s}^{-1}$, corresponding to $M_B = -24.5$. Using the Elvis et al. (1994) quasar template, the mid-IR and X-ray depth of our survey correspond to optical luminosities of $L_{\text{AGN}}^* + 1$ ($M_B = -23.5$). Therefore, we plot in Fig. 2 the cosmic evolution of optically-selected field quasars brighter than $L_{\text{AGN}}^* + 1$ ($M_B = -23.5$) and L_{AGN}^* ($M_B = -24.5$). We find a more pronounced cosmic evolution in the relative density of cluster AGN compared to the field from $z = 0$ to 1.5. In particular, the field-corrected X-ray selected AGN density in clusters evolves at least three times more rapidly than that of the field population.

This work shows that a higher surface density of AGN is observed in galaxy cluster centers than in the field and that this AGN overdensity increases with redshift out to $z \geq 1$. We therefore confirm a Butcher-Oemler type effect for AGN in galaxy clusters (e.g., Martini et al. 2007) as the number of AGN in clusters increases with redshift similar to the way that higher redshift galaxy clusters have larger numbers of blue, star-forming galaxies.

We find that up to ten percent of the galaxy clusters have at least one AGN near their center ($r < 0.25$ Mpc). Table 2 summarizes the percentage of galaxy clusters with an AGN for each selection technique and redshift bin. These fractions are field-corrected. Considering the luminosity cuts applied for each selection, only 3% of galaxy clusters at $z < 0.5$ have a radio-selected AGN near their center ($r < 0.25$ Mpc) and neither mid-IR nor X-ray selected AGN are found. We find that the fraction of galaxy clusters hosting such an AGN evolves with redshift. By $z \sim 1.5$, up to 10% of our clusters sample host at least one X-ray emitting AGN near their center (9% for radio-selected AGN).

Finally, we note that the current analysis is rather simple, using only the apparent two dimensional distribution of sources across the sky to address the evolving role of AGN in clusters. In principle, a three dimensional analysis, accounting for source redshifts (either spectroscopic or photometric), would significantly lower the field counts in each redshift bin and provide a

more robust measurement of the AGN Butcher-Oemler effect. We have opted for the former analysis as it relies only on the simple observables of position and flux, and is thus model free. Brodwin et al. (2006) derive photometric redshifts for the Boötes field AGN with an accuracy $\sigma = 0.12(1 + z)$, with a 5% outlier fraction. This is approximately half the precision that can be derived for normal galaxies. We are currently obtaining spectroscopic observations of candidate active members of clusters. Future work will use these results to better constrain the pronounced cosmic evolution of AGN activity in rich environments.

5. SUMMARY

The spatial distribution of AGN has been derived for a well-defined sample of galaxy clusters at $0 < z \leq 1.5$. The AGN are selected using three different selection techniques (mid-IR color, radio luminosity, and X-ray luminosity) that isolate distinct types of active galaxies to ensure the fullest selection of AGN in our galaxy cluster sample. An overdensity of AGN is found near the center ($r < 0.5$ Mpc) of galaxy clusters at $z > 0.5$ and this AGN excess increases with redshift. We confirm that the rising number of AGN is not simply due to the clusters becoming richer with redshift with a non-evolving fraction of cluster members being active. It is well known that AGN are also more common at high redshift. We therefore also confirm that the observed increase in redshift is more pronounced in the galaxy cluster sample than in the field. We thus find a Butcher-Oemler type effect for AGN in galaxy clusters.

We thank the anonymous referee whose comments significantly improved this paper. We thank Joel Vernet and Carlos De Breuck for carefully reading the manuscript. This work is partly based on observations made with the *Spitzer Space Telescope*, which is operated by the Jet Propulsion Laboratory, California Institute of Technology under a contract with NASA. This work made use of data products provided by the NOAO Deep Wide-Field Survey, which is supported by the National Optical Astronomy Observatory (NOAO). NOAO is operated by AURA, Inc., under a cooperative agreement with the National Science Foundation. AHG acknowledges support from NSF grant AST-0708490. SAS's work was performed under the auspices of the U.S. Department of Energy, National Nuclear Security Administration by the University of California, Lawrence Livermore National Laboratory under contract No. W-7405-Eng-48.

³ Croom et al. (2004) present various forms of the empirical QLF. We use the version which fits the QLF with a second-order polynomial to describe the luminosity evolution (Table 5 of that paper).

REFERENCES

- Bahcall, J. N., Schmidt, M., & Gunn, J. E. 1969, *ApJ*, 157, L77
- Becker, R. H., White, R. L., & Helfand, D. J. 1995, *ApJ*, 450, 559
- Best, P. N., Kauffmann, G., Heckman, T. M., Brinchmann, J., Charlot, S., Ivezić, Z., & White, S. D. M. 2005, *MNRAS*, 362, 25
- Bignamini, A., Tozzi, P., Borgani, S., Ettori, S., & Rosati, P. 2008, *A&A*, 807
- Birzan, L., Rafferty, D. A., McNamara, B. R., Wise, M. W., & Nulsen, P. E. J. 2004, *ApJ*, 607, 800
- Brand, K. et al. 2006, *ApJ*, 641, 140
- Brodwin, M., Gonzalez, A. H., Moustakas, L. A., Eisenhardt, P. R., Stanford, S. A., Stern, D., & Brown, M. J. I. 2007, *ApJ*, 671, L93
- Brodwin, M. et al. 2006, *ApJ*, 651, 791
- . 2008, *astro-ph*: arXiv0810.0528
- Brown, M. J. I. et al. 2006, *ApJ*, 638, 88
- Cappi, M. et al. 2001, *ApJ*, 548, 624
- Coil, A. L., Hennawi, J. F., Newman, J. A., Cooper, M. C., & Davis, M. 2007, *ApJ*, 654, 115
- Condon, J. J. 1992, *ARA&A*, 30, 575
- Condon, J. J., Cotton, W. D., Greisen, E. W., Yin, Q. F., Perley, R. A., Taylor, G. B., & Broderick, J. J. 1998, *AJ*, 115, 1693
- Croft, S., de Vries, W., & Becker, R. H. 2007, *ApJ*, 667, L13
- Croom, S. M., Smith, R. J., Boyle, B. J., Shanks, T., Miller, L., Outram, P. J., & Loaring, N. S. 2004, *MNRAS*, 349, 1397
- Croom, S. M. et al. 2005, *MNRAS*, 356, 415
- de Vries, W. H., Morganti, R., Röttgering, H. J. A., Vermeulen, R., van Breugel, W., Rengelink, R., & Jarvis, M. J. 2002, *AJ*, 123, 1784
- Dey, A. et al. 2008, *ApJ*, 677, 943
- Dickinson, M. 1993, in *Astronomical Society of the Pacific Conference Series*, Vol. 51, *Observational Cosmology*, ed. G. L. Chincarini, A. Iovino, T. Maccacaro, & D. Maccagni, 434
- Donley, J. L., Rieke, G. H., Perez-Gonzalez, P. G., & Barro, G. 2008, *astro-ph*: arXiv:0806.4610
- Dressler, A., Thompson, I. B., & Shectman, S. A. 1985, *ApJ*, 288, 481
- Dunlop, J. S. & Peacock, J. A. 1990, *MNRAS*, 247, 19
- Eastman, J., Martini, P., Sivakoff, G., Kelson, D. D., Mulchaey, J. S., & Tran, K.-V. 2007, *ApJ*, 664, L9
- Ebeling, H., Edge, A. C., & Henry, J. P. 2001, *ApJ*, 553, 668
- Eckart, M. E., Stern, D., Helfand, D. J., Harrison, F. A., Mao, P. H., & Yost, S. A. 2006, *ApJS*, 165, 19
- Eisenhardt, P. R. et al. 2004, *ApJS*, 154, 48
- Eisenhardt, P. R. M. et al. 2008, *ApJ*, 684, 905
- Elston, R. J. et al. 2006, *ApJ*, 639, 816
- Elvis, M. et al. 1994, *ApJS*, 95, 1
- Gehrels, N. 1986, *ApJ*, 303, 336
- Gorjian et al. 2008, *ApJ*, 679
- Gunn, J. & Weinberg, D. 1995, in *Wide Field Spectroscopy and the Distant Universe*, ed. S. J. Maddox & A. Aragon-Salamanca, 3
- Jannuzi, B. T. & Dey, A. 1999, in *Astronomical Society of the Pacific Conference Series*, Vol. 191, *Photometric Redshifts and the Detection of High Redshift Galaxies*, ed. R. Weymann, L. Storrie-Lombardi, M. Sawicki, & R. Brunner, 111
- Kenter, A. et al. 2005, *ApJS*, 161, 9
- Lacy, M. et al. 2004, *ApJS*, 154, 166
- Lin, Y.-T. & Mohr, J. J. 2007, *ApJS*, 170, 71
- Magliocchetti, M. et al. 2008, *MNRAS*, 383, 1131
- Magorrian, J. et al. 1998, *AJ*, 115, 2285
- Martini, P., Kelson, D. D., Kim, E., Mulchaey, J. S., & Athey, A. A. 2006, *ApJ*, 644, 116
- Martini, P., Kelson, D. D., Mulchaey, J. S., & Trager, S. C. 2002, *ApJ*, 576, L109
- Martini, P., Mulchaey, J. S., & Kelson, D. D. 2007, *ApJ*, 664, 761
- Matthews, T. A., Morgan, W. W., & Schmidt, M. 1964, *ApJ*, 140, 35
- McNamara, B. R. et al. 2000, *ApJ*, 534, L135
- Miley, G. K. et al. 2004, *Nature*, 427, 47
- Murray, S. S. et al. 2005, *ApJS*, 161, 1
- Pope, A., Chary, R., Dickinson, M., & Scott, D. 2006, in *Bulletin of the American Astronomical Society*, Vol. 38, *Bulletin of the American Astronomical Society*, 1172
- Richards, G. T. et al. 2006, *ApJS*, 166, 470
- Ruderman, J. T. & Ebeling, H. 2005, *ApJ*, 623, L81
- Schmidt, M. 1968, *ApJ*, 151, 393
- Serjeant, S., Gruppioni, C., & Oliver, S. 2002, *MNRAS*, 330, 621
- Stanford, S. A. et al. 2005, *ApJ*, 634, L129
- Stern, D., Djorgovski, S. G., Perley, R. A., de Carvalho, R. R., & Wall, J. V. 2000, *AJ*, 119, 1526
- Stern, D., Holden, B., Stanford, S. A., & Spinrad, H. 2003, *AJ*, 125, 2759
- Stern, D. et al. 2005, *ApJ*, 631, 163
- Ueda, Y., Akiyama, M., Ohta, K., & Miyaji, T. 2003, *ApJ*, 598, 886
- Venemans, B. P. et al. 2005, *A&A*, 431, 793
- . 2007, *A&A*, 461, 823

TABLE 1
NUMBER AND SURFACE DENSITY OF BOÖTES AGN CANDIDATES AFTER LUMINOSITY CUTS.

Selection	Luminosity limit (ergs s ⁻¹)	Area (deg ²)	Total number N (Σ , arcmin ⁻²)	0 < z ≤ 0.5 N _{AGN} (Σ_{AGN})	0.5 < z ≤ 1 N _{AGN} (Σ_{AGN})	1 < z ≤ 1.5 N _{AGN} (Σ_{AGN})
Mid-IR	$S_{5.8\mu\text{m}} > 2.2 \times 10^{44}$	8.0	2262 (0.079)	177 (0.006)	1570 (0.054)	2262 (0.079)
Radio	$S_{1.4\text{GHz}} > 2.5 \times 10^{40}$	6.68	3172 (0.132)	229 (0.009)	591 (0.025)	1394 (0.058)
X-ray	$S_{0.5-7\text{keV}} > 3.3 \times 10^{43}$	9.0	3293 (0.102)	205 (0.006)	2102 (0.065)	3293 (0.102)

TABLE 2
FRACTION OF GALAXY CLUSTERS WITH AT LEAST ONE
AGN IN THE INNER 0.25 MPC

Selection	0 < z ≤ 0.5	0.5 < z ≤ 1	1 < z ≤ 1.5
Mid-IR	< 1%	5 ± 2%	4 ± 3%
Radio	3 ± 2%	8 ± 3%	9 ± 4%
X-ray	< 1%	3 ± 2%	10 ± 4%

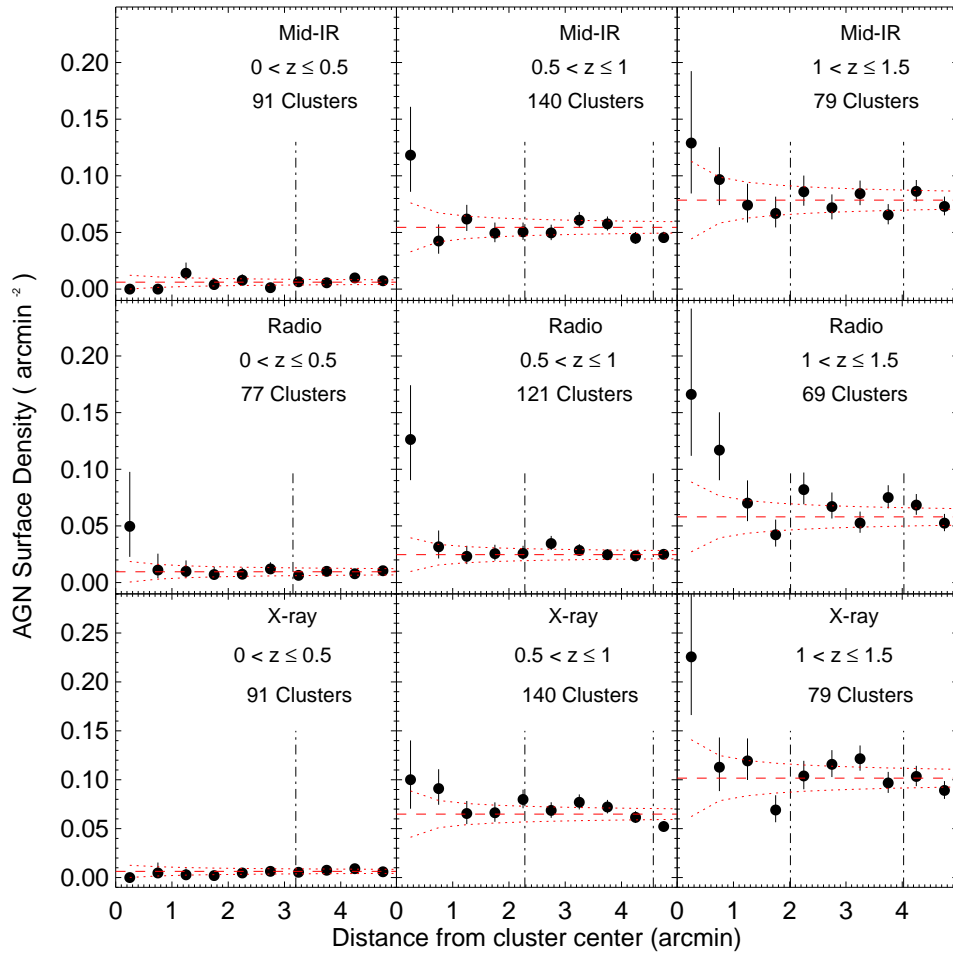


FIG. 1.— Radial density profile of mid-IR selected AGN (top row), radio-selected AGN (middle row) and X-ray selected AGN (bottom row). Galaxy clusters are divided into three redshift bins: $z \leq 0.5$ (left column), $0.5 < z \leq 1$ (middle column) and $1 < z \leq 1.5$ (right column). The global field density is shown by the red dashed line. The red dotted lines indicate the 1σ variations in the field densities and the error bars indicate the 1σ errors on the AGN counts; both assume Poissonian errors and Gehrels (1986) small numbers approximation. The 1 Mpc and 2 Mpc projected radii are indicated by vertical dot-dashed lines for the median redshift of the clusters plotted in each bin. The number of galaxy clusters used in the profile calculation is also indicated at the top right of each panel. An overdensity of AGN is observed in the centers of galaxy clusters at $z > 0.5$ while little or no variation relative to the field density is found at lower redshifts ($z \leq 0.5$).

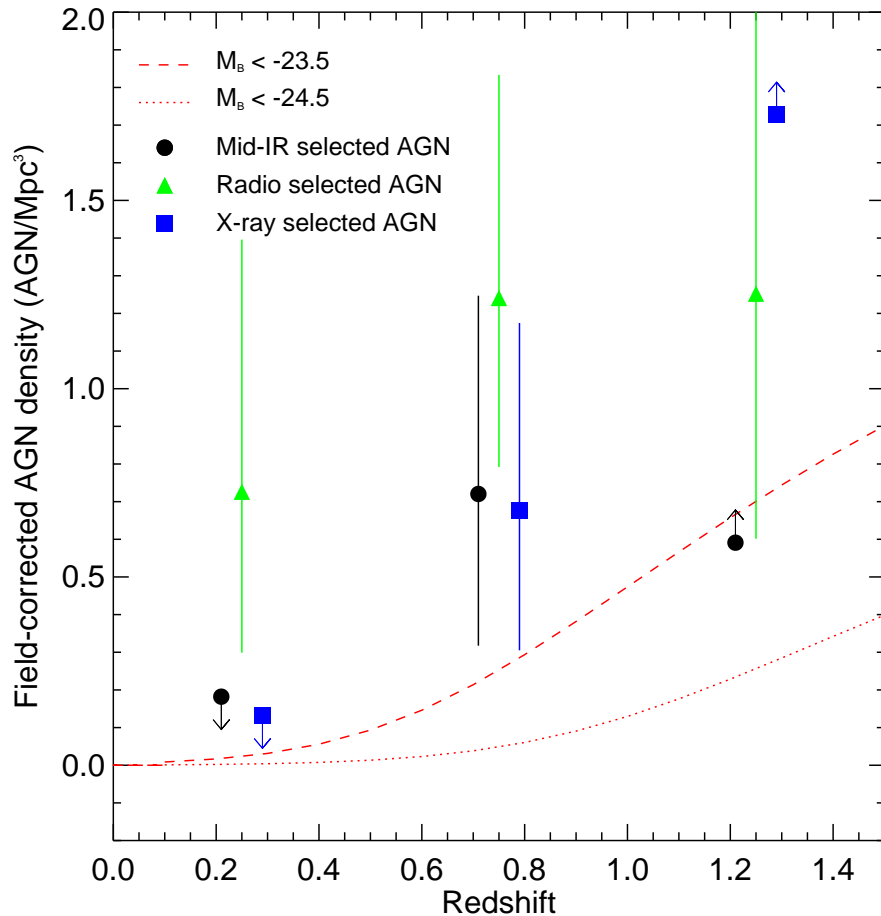


FIG. 2.— Field-corrected volume density of AGN in galaxy clusters and comparison of its evolution relative to an optical quasar luminosity function. Points show the field-corrected overdensity of AGN within 0.25 Mpc of the ISS cluster centers for the three AGN criteria: mid-infrared (black points), radio (green triangles) and X-ray (blue squares). No mid-IR or X-ray selected AGN are found within 0.25 Mpc for the galaxy clusters at $z < 0.5$. We plot the 1σ uncertainty of the field density as an upper limit. Lines show the relative evolution of quasars brighter than L_{AGN}^* ($M_B = -24.5$, dotted red line) and $L_{\text{AGN}}^* + 1$ ($M_B = -23.5$, dashed red line) for the field, where L_{AGN}^* is calculated at $z = 1$. These models, which show a less dramatic evolution of AGN in the field relative to clusters, are calculated from the Croom et al. (2004) 2dFQZ QLF (see text for details).